

NGHT-1X Pole Cover Erosion Measurements on Xenon and Krypton

Alex W. Nikrant¹, Zachary Switzer², Michael J. Glogowski³
Northrop Grumman Space Systems, Dulles, VA 20166, USA

Gabriel F. Benavides⁴, Matthew J. Baird⁵, Jonathan A. Mackey⁶
National Aeronautics and Space Administration Glenn Research Center, Cleveland, OH 44135, USA

Northrop Grumman's NGHT-1X Hall thruster has completed the Engineering Model development phase and is progressing towards qualification and flight unit build and test. First flight of the NGHT-1X will occur in 2025 on Northrop Grumman's Mission Extension Pod spacecraft. The NGHT-1X is a state of the art 1 kW-class Hall thruster which implements magnetic shielding to increase thruster lifetime by reducing discharge channel wall erosion. As a result, like other magnetically shielded Hall thrusters, the NGHT-1X exhibits erosion of the front-facing pole covers, which is the primary life-limiting failure mode of the thruster. During the development of the NGHT-1X, several Short Duration Wear Tests were performed to characterize erosion rates and forecast compliance to lifetime requirements in advance of the ongoing full-life Long Duration Wear Test. Erosion rate measurements from four tests at different operating conditions are presented and comparisons made between tests. Two tests were performed in the same background pressure environment at 700 W 300 V and 900 W 350 V throttle conditions, both using xenon propellant. A third test was performed again at 900 W 350 V with xenon propellant, but at a lower background pressure. Lastly, to assess the viability of potential future applications with alternate propellants, a wear test was conducted using krypton propellant at 900 W 250 V, the results of which are presented here. The erosion measurements from each test are compared with one another, and insights are discussed. All xenon wear tests support a thruster lifetime capability in excess of 16,000 hours, or 3.3 MNS at 900 W 350 V, which supports the Mission Extension Pod mission with margin as well as many other potential applications on small- to medium-sized spacecraft.

I. Introduction

Northrop Grumman's NGHT-1X Hall thruster [1] has completed the Engineering Model (EM) development phase and is progressing towards qualification and flight unit build and test. First flight of the NGHT-1X will occur on the Mission Extension Pod (MEP) in 2025. The NGHT-1X, which is based on NASA Glenn Research Center's (GRC) H71M thruster [2,3] via a license to GRC's small spacecraft electric propulsion technology suite, is a state of the art 1 kW-class Hall thruster which implements magnetic shielding to increase thruster lifetime. Since its initial discovery during wear

1. Principal Mechanical Engineer, Propulsion Engineering Department, Alex.Nikrant@ngc.com, AIAA Member.
2. Principal Mechanical Engineer, Propulsion Engineering Department, Zachary.Switzer@ngc.com.
3. NG Fellow, Michael.Glogowski@ngc.com, AIAA Senior Member.
4. Senior Research Engineer, Electric Propulsion System Branch, AIAA Senior Member.
5. Research Engineer, Electric Propulsion System Branch.
6. Research Engineer, Electric Propulsion System Branch.

testing of the BPT-4000 [4,5], magnetic shielding has become increasingly popular as a method to increase the lifetime of Hall thrusters by substantially reducing the erosion of the discharge channel.

In unshielded thrusters, the discharge channel walls erode away until the metal components of the magnetic circuit are exposed to the discharge plasma, which typically occurs after several thousand hours. These metal parts subsequently erode away at a much faster rate, ultimately leading to thruster failure not long afterwards. By shaping the magnetic field lines to follow the contour of the discharge channel walls, the walls eventually reach a zero-erosion erosion state which can protect the underlying metal components from the plasma indefinitely, eliminating the primary failure mode of conventional Hall thrusters [5].

However, magnetic shielding has been found to have unintended consequences. While discharge channel erosion is significantly reduced and even eliminated entirely, early testing revealed previously unobserved erosion occurring on the front faces of the thruster [6]. This is partly due to the fact that a magnetically shielded field topology pushes the discharge plasma further downstream, providing a more direct view from the plasma to front-facing thruster surfaces [7]. In fact, wear testing of the HERMeS 12.5 kW thruster shows that a “more magnetically shielded” topology, i.e., one which pushes the peak magnetic field further downstream, results in higher pole cover erosion rates [8], suggesting that a proper balance is key to maximizing thruster lifetime. Still, magnetic shielding has been found superior to conventional unshielded designs, as the pole erosion can be managed by the inclusion of pole covers made from low-sputter-yield materials such as aluminum oxide (alumina) or graphite, enabling lifetimes in excess of 10,000 hours [6].

At present, the mechanisms which drive pole cover erosion are not understood well enough to develop fully predictive simulations. While significant progress towards that goal has been made in recent years, simulations still require heavy correlation to test data, and even then, they still do not replicate observed erosion patterns exactly [6,7,9,10]. Additionally, testing of Hall thrusters such as HERMeS/AEPS and MaSMi have demonstrated counterintuitive trends in erosion behavior, such as increased erosion rates at decreased discharge current and/or voltage [11,12,13]. As a result, it is currently impossible to accurately predict the erosion rate and resulting lifetime capability of a magnetically shielded Hall thruster without first designing, building, and testing it.

Therefore, as part of the NGHT-1X EM development phase, Northrop Grumman (NG) performed four Short Duration Wear Tests (SDWTs) to characterize via test the erosion rates of the Inner and Outer Front Pole Covers (IFPC, OFPC) during thruster firing at various operating conditions. The results of these SDWTs are presented and discussed in this paper. Of the four SDWTs performed, one was performed using krypton propellant. To the knowledge of the authors, this represents the first publication of pole cover erosion rate measurements in a magnetically shielded Hall thruster using krypton propellant.

In Section II, experimental methods are discussed including thrusters, test facilities, and erosion measurement techniques used. Section III presents the wear test results, while Section IV contains discussions and comparisons of the results. Conclusions are found in Section V.

II. Experimental Method

A. Summary of Wear Tests Performed

A summary of the SDWTs performed on the NGHT-1X is presented in Table 1. These SDWTs are listed in chronological order and occurred between March 2022 and April 2023. For all xenon SDWTs, the magnetic field was set at the strength that yielded optimal performance for each throttle condition, which varied slightly between 700 W 300 V and 900 W 350 V. SDWT-2 and SDWT-3 used the same magnetic field strength; the only difference in test parameters was the facility and the resulting background pressure.

NG performed the krypton SDWT to assess the lifetime capability of the NGHT-1X on krypton for potential mission applications outside of MEP. Because this SDWT is not relevant to MEP and uses krypton propellant, it is referred to as SDWT-Kr rather than SDWT-4. This SDWT utilized a lower discharge voltage due to increased thermal loading associated with operation on krypton propellant.

Table 1. Summary of Wear Tests Performed.

Test Name	Unit Under Test	Facility	Propellant	Throttle Condition	Duration	Background Pressure
SDWT-1	EM1	VF-8	Xenon	700 W 300 V	500 hours	11 μ torr-Xe
SDWT-2	EM1	VF-8	Xenon	900 W 350 V	464 hours	12 μ torr-Xe
SDWT-3	EM2R	VF-11	Xenon	900 W 350 V	501 hours	5 μ torr-Xe
SDWT-Kr	EM1R	VF-11	Krypton	900 W 250 V	290 hours	7 μ torr-Kr

B. Thrusters

The first two SDWTs utilized the first NGHT-1X EM thruster built by NG, EM1. At the time of SDWT-1, EM1 had undergone approximately 50 hours of operation between an initial performance characterization and integrated testing with an EM PPU, meaning the thruster’s discharge channel and pole covers represented Beginning of Life (BOL) conditions. This same unit went on to perform a number of other tests and had accumulated approximately 600 hours of operation by the start of SDWT-2.

The only new parts for SDWT-2 were the pole covers; all SDWTs utilized new, polished pole covers in order to obtain the most accurate erosion measurements. For SDWTs 2, 3, and Kr, the pole covers also featured chamfered edges to simulate a more worn-in condition. Only SDWT-1 used non-chamfered pole covers, which demonstrated that the pole cover edges are eroded away by beam ions within the first several hundred hours of operation.

SDWT-3 utilized a second thruster, referred to as EM2R, where the R signifies “rebuilt”. The original EM2 thruster performed a series of tests focusing on structural performance, as described in [1]. After these structural tests, NG replaced several components (not related to any issues during structural tests), and accordingly updated the thruster designation to EM2R. Magnet mapping and flow symmetry testing was performed for both the EM1 and EM2R magnetic circuits and anode assemblies, respectively. Both thrusters showed high degrees of symmetry – less than $\pm 1\%$ variation in peak magnetic field strength and less than $\pm 2\%$ variation in flow distribution within the discharge channel – and very close agreement between thrusters. Therefore, erosion rate variation due to unit build differences is expected to be small, if not negligible.

One of the replaced components was the discharge channel, which in EM2R was pre-machined to represent the discharge channel profile measured at the end of SDWT-1, i.e., the beginning of SDWT-2. This was done in order to draw the best comparison between the erosion results of SDWT-2 and SDWT-3, which occurred at the same throttle condition but at different background pressures. The SDWT-3 pole cover chamfers also matched the profile measured at the end of SDWT-1.

After completing SDWT-2, NG rebuilt the EM1 thruster with a new discharge channel prior to the krypton SDWT, earning the designation EM1R. Like SDWTs 2 and 3, the discharge channel and pole covers used in SDWT-Kr represented a “worn in” geometry, accomplished by machining certain edges of the parts to represent some amount of erosion.

C. Test Facilities

The first two SDWTs performed on the NGHT-1X occurred in NASA GRC’s Vacuum Facility (VF) 8 chamber. VF-8 is a 1.5-m diameter, 4.5-m long vacuum chamber which has a pumping speed of 120,000 L/s on N₂ and a base pressure of 7×10^{-8} torr. During SDWTs 1 and 2, facility background pressure was 11 and 12 μ torr-Xe, respectively, measured on the side wall of the facility.

The latter two SDWTs occurred in NASA GRC’s VF-11 facility, which is larger than VF-8 at 2.2-m in diameter and 8.25-m in length. VF-11 also has a higher pumping speed than VF-8 at 270,000 L/s on N₂, with a base pressure of 10^{-7} torr. In VF-11, in addition to a vacuum gauge on the side wall of the facility, background pressure is also measured on an ion gauge positioned coplanar with the thruster near the thrust stand. During SDWT-3, facility background pressure measured near the thruster was 5 μ torr-Xe. Unfortunately, the ion gauge near the thruster was not connected properly during the krypton SDWT. Based on measurements at the facility side wall at different throttle conditions and comparing to past tests in VF-11, it is estimated that the ion gauge near the thruster would have measured 7 μ torr-Kr during the

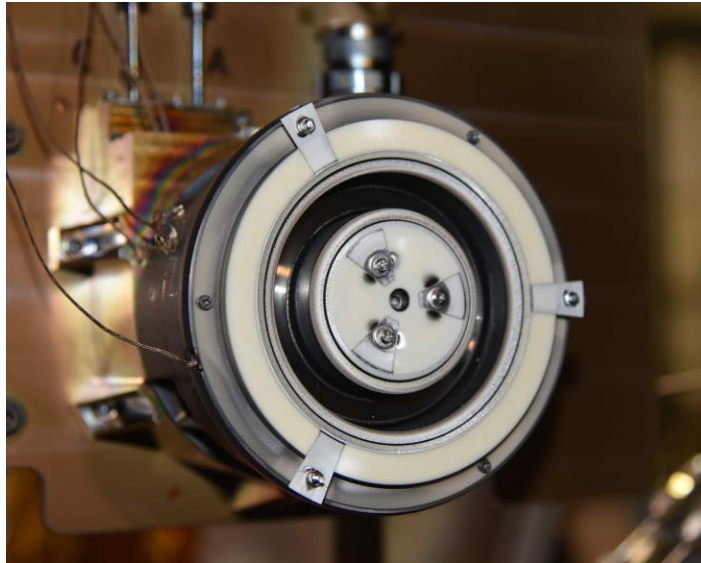


Figure 1. The EM2R thruster following SDWT-3 in VF-11.

SDWT. VF-11 is equipped with a Faraday and Langmuir probe package on a rotating probe arm, though no plume data is presented in this paper.

Background material deposition rates for both facilities were characterized at different points throughout the NGHT-1X test campaign but not for every SDWT performed. In all cases, deposition rates were on the order of 1-2 $\mu\text{m}/\text{hr}$, which is one to two orders of magnitude lower than the measured erosion. Therefore, in this paper, no correction for material deposition is applied when calculating erosion rates.

In all tests, a set of DC power supplies controlled the thruster discharge, electromagnets, cathode heater, and cathode keeper. Two mass flow controllers set the flow rates through the anode and cathode independently; however, during testing, the cathode flow was always set to the same percentage of the anode flow at all conditions to mimic the nominal cathode flow fraction determined by the Xenon Flow Controller (XFC). The flow controllers are calibrated and have an uncertainty of approximately $\pm 1.0\%$ of the setpoint. Both facilities are equipped with thrust stands, but thrust data is not presented in this paper.

D. Erosion Measurements

Two methods for characterizing erosion were employed across the four SDWTs discussed in this paper. For all SDWTs performed, thin alumina masks were installed at three locations on both the Inner Front Pole Cover (IFPC) and Outer Front Pole Cover (OFPC). This method is described in detail in [14] and has been employed extensively during the 12.5 kW HERMeS/AEPS thruster development program [12,15]. The same method has also been used on smaller thrusters such as MaSMi [13]. The masks protect an underlying portion of the pole cover surface during the SDWT, which provides an uneroded reference surface when making post-test measurements. Each post-test pole cover is scanned with a surface profilometer in the azimuthal direction at multiple radii, and the step height between eroded and uneroded surfaces is used in conjunction with the test duration to calculate the erosion rate at that radius. An example of the NGHT-1X with masks installed is shown in Figure 1, which depicts the EM2R thruster following the third SDWT in VF-11. (The fastener erosion and metal deposition visible on the IFPC is discussed in a later section.) In order to obtain the best measurement possible, all pole covers were polished prior to each SDWT, and the tests lasted several hundred hours to allow for a sufficiently measurable amount of net erosion.

In addition to the masking method, erosion rates for each test were calculated by subtracting out pre- and post-test radial profilometer scans. Whereas the masking method is backed by a thorough uncertainty analysis considering factors such as part warpage and roughness [14], no in-depth uncertainty analysis has been performed for the scan subtraction method for the results presented here. Initially, calculations using the subtraction method were intended only for reference, assuming that the masking method provided more accurate results. However, performing both measurement techniques over multiple tests has revealed a consistent discrepancy between the two methods, which is one of the main

points of discussion in the following section.

All profilometer measurements for the masking method were collected on a Nanovea ST-400 profilometer. Masking method results are only presented for SDWTs 1, 2, and 3; performing the same masking analysis on the krypton SDWT was deemed unnecessary due to the extremely high erosion rates observed, so only the subtraction method is presented for SDWT-Kr. Masks for all tests are at the 3, 7, and 11 o'clock positions of both the IFPC and OFPC (see Figure 1), where 12 o'clock is defined as the upward direction in the mounted test configuration.

For the subtraction method, surface data consisted of radial scans along different angles across the surface of the pole covers. These are typically done along three different axes (2-6 o'clock, 4-10 o'clock, and 6-12 o'clock), though SDWT-3 and SDWT-Kr differ and are discussed further in a later section. The NGHT-1X OFPC features a step around the full circumference which provides a reference surface that does not experience any erosion during testing. This step is used to align pre- and post-test scans before subtracting them to calculate erosion.

For SDWTs 1 and 2, the same Nanovea ST-400 generated the data used for the subtraction method. Obtaining these measurements on the Nanovea required individual radial scans along the three axes of interest. In the middle of the NGHT-1X test campaign, NASA GRC obtained a Keyence VRX-6000 profilometer which collects data across the entire surface of the pole covers in a shorter period of time than the Nanovea. While the Nanovea continued to provide data for the masking method, the Keyence profilometer was used to calculate erosion via the subtraction method for SDWT-3 and SDWT-Kr. The Keyence profilometer generates a 3D map of the surface in a single scan, meaning the radial "scans" are simply 2D slices of the 3D scan generated in the Keyence software.

Erosion rates in all plots are presented as real erosion rate in microns per thousand hours ($\mu\text{m}/\text{KHR}$) of firing time over a normalized spatial dimension. For the IFPC, $R = 0$ corresponds to the inner edge of the pole cover hole at the centrally mounted cathode, while $R = 1$ corresponds to the edge of the pole cover adjacent to the discharge channel. For the OFPC, $R = 0$ corresponds to the edge adjacent to the discharge channel and $R = 1$ represents the edge of the pole cover prior to the step down to the lower ledge which contains the fasteners (see Figure 1).

III. Wear Test Results

A. Xenon Erosion Rates from the Masking Method

Xenon erosion rates calculated with the masking method for SDWT-1 (700 W 300 V, 11 $\mu\text{torr-Xe}$) are shown in Figure 2; SDWT-2 (900 W 350 V, 12 $\mu\text{torr-Xe}$) in Figure 3; and SDWT-3 (900 W 350 V, 5 $\mu\text{torr-Xe}$) in Figure 4. In each plot, the number in the legend indicates the "o'clock" direction corresponding to the data.

Erosion data from SDWT-1 is more sparse than data from the later SDWTs. As mentioned earlier, for the masking method, a full azimuthal scan is performed at each radius where a measurement is to be made. This is a time-consuming process, so initially fewer data was collected. However, for subsequent tests it was deemed worth it to spend additional time (several hours) to collect a higher density of erosion measurements.

Additionally, the calculated erosion rates from SDWT-1 were impacted by net material deposition around the edges and underneath the masks. Due to design limitations affecting the ability to install the masks, the masks were suspended above the surface by an estimated .001-.002 inches, which was enough to allow collection of backsputtered graphite from the test facility to accumulate underneath the masks near the edges. The surface underneath the center of the masks was left pristine, so measurements were still possible in most cases, but the measurement uncertainty is driven up as a result. Attempts were made to improve mask installation during setup for SDWT-2 and SDWT-3, which reduced material accumulation but did not eliminate it completely.

The gap in data between $R = 0.25$ and $R = 0.6$ on the IFPC in all tests is due to the IFPC fasteners, which prevent a clear measurement. Additionally, the masks did not provide coverage all the way to the edges of the pole covers. This was done intentionally, in order to prevent any undesirable plasma interactions with the edges of the masks. On the IFPC, this means a lack of data below $R = 0.1$ and above $R = 0.8-0.9$. The OFPC masking arrangement allowed measurement all the way to $R=1$ because of the step-down feature of the part, but there is no data below $R = 0.2$ for the OFPC.

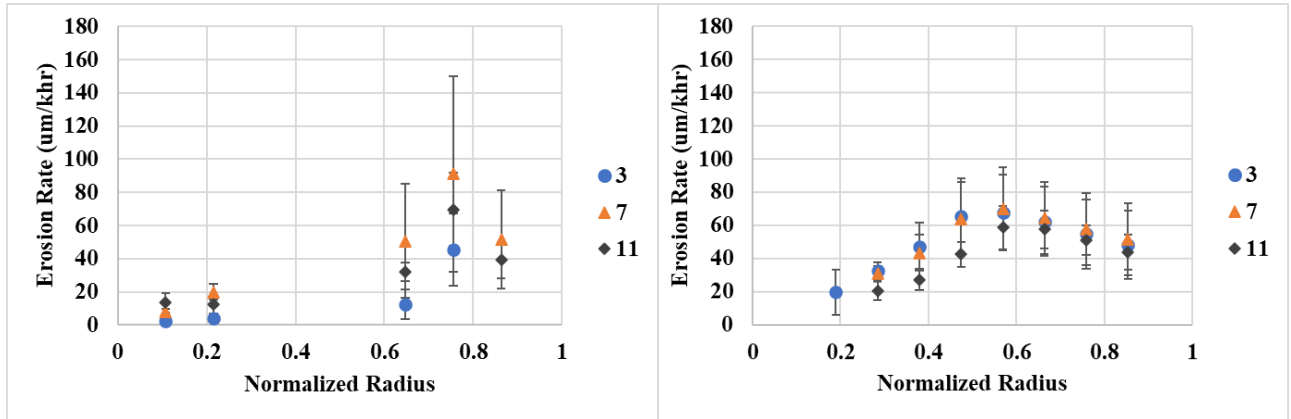


Figure 2. Masking method erosion rates for SDWT-1 (700 W 300 V, 11 μtorr-Xe). Left: IFPC, Right: OFPC.

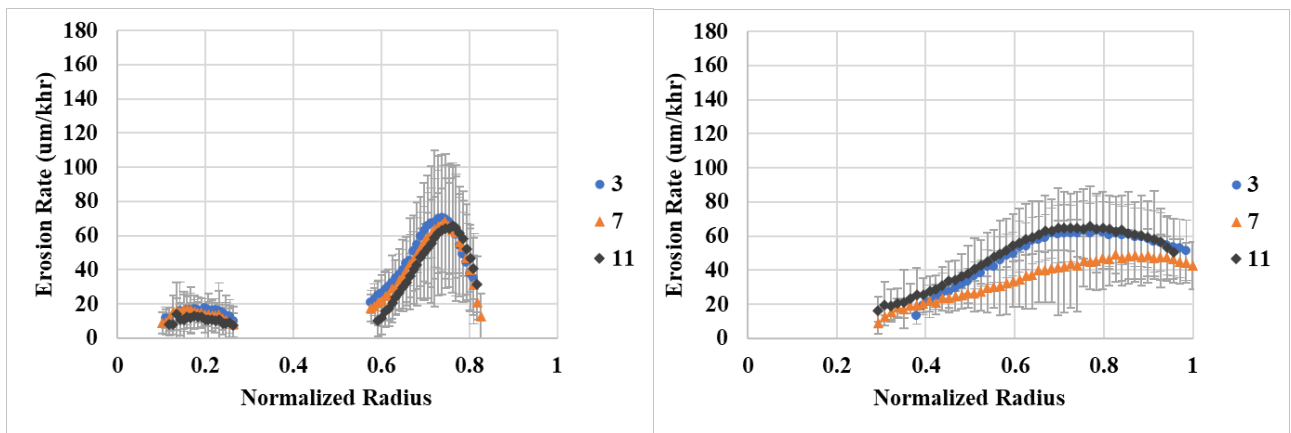


Figure 3. Masking method erosion rates for SDWT-2 (900 W 350 V, 12 μtorr-Xe). Left: IFPC, Right: OFPC.

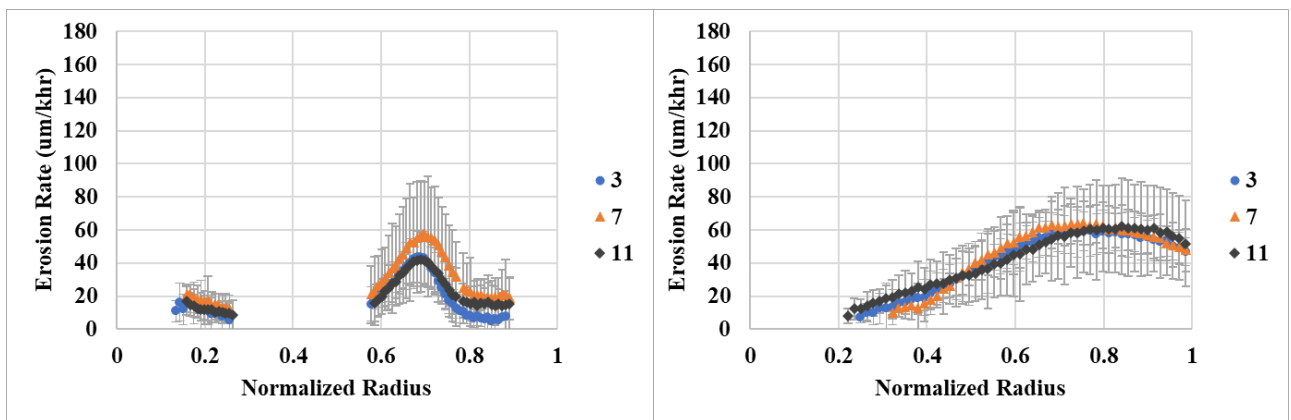


Figure 4. Masking method erosion rates for SDWT-3 (900 W 350 V, 5 μtorr-Xe). Left: IFPC, Right: OFPC.

B. Xenon Erosion Rates from the Subtraction Method

Xenon erosion rates calculated with the subtraction method for SDWT-1 (700 W 300 V, 11 μ torr-Xe) are shown in Figure 5; SDWT-2 (900 W 350 V, 12 μ torr-Xe) in Figure 6; and SDWT-3 (900 W 350 V, 5 μ torr-Xe) in Figure 7. In each plot, the number in the legend indicates the “o’clock” direction corresponding to the data.

The subtraction method was not part of the original test plan at the beginning of the NGHT-1X test campaign, and therefore there were no pre-test radial scans performed prior to SDWT-1. To calculate erosion rates via the subtraction method for SDWT-1, the nominal design dimensions are used for the pre-test surface. The variation over different angles in the SDWT-1 data, particularly evident on the OFPC, is most likely not real variation but rather reflects non-flatness of the part that existed prior to the test, which is not accounted for when using the nominal design dimensions. Non-flatness is observed on the pre-test pole cover scans from other tests at a magnitude which would explain the observed variation in OFPC erosion rates in Figure 5.

In addition to the issue of non-flatness, this approach does not take into account the possibility that the heights of the IFPC and OFPC may have varied from the nominal dimensions within their tolerance ranges. The method of calculation combined with the dimensional tolerances of the IFPC and OFPC could allow for up to $\pm 100 \mu\text{m}/\text{hr}$ of linear offset of the entire erosion profile. For this reason, the subtraction method results for SDWT-1 in terms of absolute erosion rate should be taken with a grain of salt, but the data still provides useful insight regarding the overall erosion distribution, in particular the relative size of the IFPC erosion peak with respect to the lower erosion in other areas.

As mentioned previously, erosion rates calculated via the subtraction method for SDWTs 1 and 2 used the Nanovea profilometer, while for SDWT-3 (and SDWT-Kr) the Keyence VRX-6000 was used. Figure 5 and Figure 6 show that the Nanovea data sets exhibit higher noise than those collected on the Keyence profilometer, which are likely due to measurement configuration settings rather than any problem with the Nanovea profilometer. For clarity, an “Average” line is calculated and displayed for SDWTs 1 and 2. While there may be some real angular variation in the erosion rates, it is dwarfed by the measurement noise. Because the noise levels from the Keyence profilometer are lower, no average line is included for SDWTs 3 and Kr.

Erosion rates along six traces are shown for SDWTs 1 and 2. Different traces are used for SDWT-3 data for two reasons. During SDWT-3 setup, in an effort to reduce the material accumulation under the masks mentioned earlier, a different fastener arrangement was used to install the IFPC masks. This resulted in more metal exposed to the plasma and led to a region of net deposition near each fastener (see Figure 1). These net-deposition regions fall along the typical trace directions presented in other plots for the subtraction method. Additionally, in the post-SDWT-3 scan, there is an anomaly in the 6-to-12 o’clock direction which occupies an approximately ± 10 degree region and artificially reduces erosion rates. It is believed that another light source in the room may have created reflections that distorted the measurements. Both the net deposition from the fasteners and the scan anomaly have clear boundaries in the post-test scan, so new trace directions were chosen to avoid both regions. These traces fall approximately in the 3, 8, and 10 o’clock directions.

Because the NGHT-1X does not begin life in a fully magnetically shielded configuration, the edges of the pole covers experience erosion from the same beam ions which erode the discharge channel. This chamfering effect can be seen in Figure 1, if you have very good eyesight. Edge-on erosion of the pole cover corners will slow down and eventually stop as the discharge channel stops eroding, after which the chamfered regions will only see erosion from the same ion populations which erode the front faces of the pole covers. For this reason, erosion rates in the chamfer regions are not shown for any of subtraction method plots, as the magnitude of the erosion rate would suggest less lifetime capability than is really the case. While discharge channel erosion is not presented in this paper, the erosion profile overlaid with the NGHT-1X magnetic field streamlines indicate that once the discharge channel stops eroding, enough of the pole cover edges will remain to support the full lifetime capability of the thruster with margin.

C. Krypton Erosion Rates

Erosion rates calculated with the subtraction method from the krypton SDWT (900 W 250 V, 7 μ torr-Kr) are presented in Figure 8.

The same potential reflection interference that is present in the SDWT-3 data is also present in the SDWT-Kr data, both taken on the Keyence VRX-6000 profilometer. Therefore, the 6 o’clock and 12 o’clock traces are excluded from the plots. Further discussion of the krypton erosion rates is found in the following section.

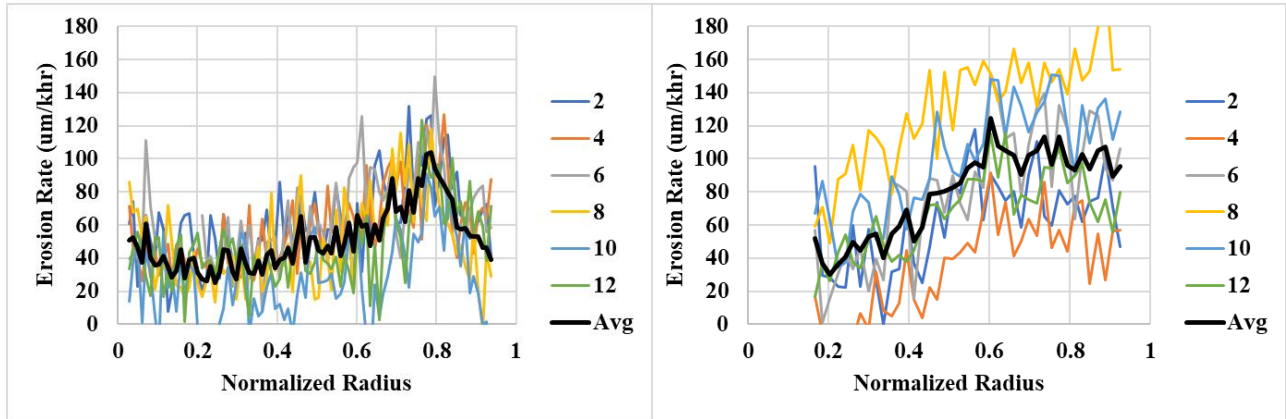


Figure 5. Subtraction method erosion rates for SDWT-1 (700 W 300 V, 11 μ torr-Xe). Left: IFPC, Right: OFPC.

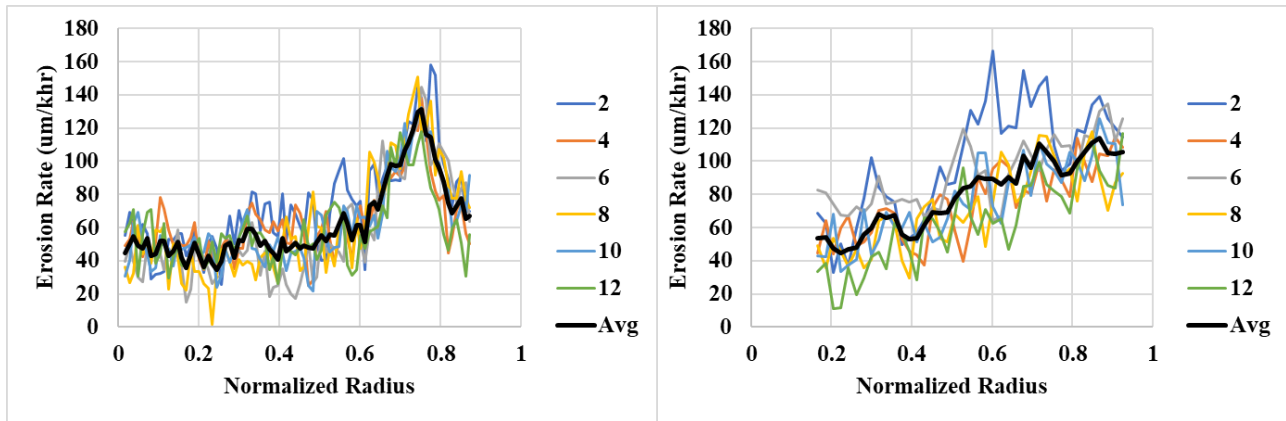


Figure 6. Subtraction method erosion rates for SDWT-2 (900 W 350 V, 12 μ torr-Xe). Left: IFPC, Right: OFPC.

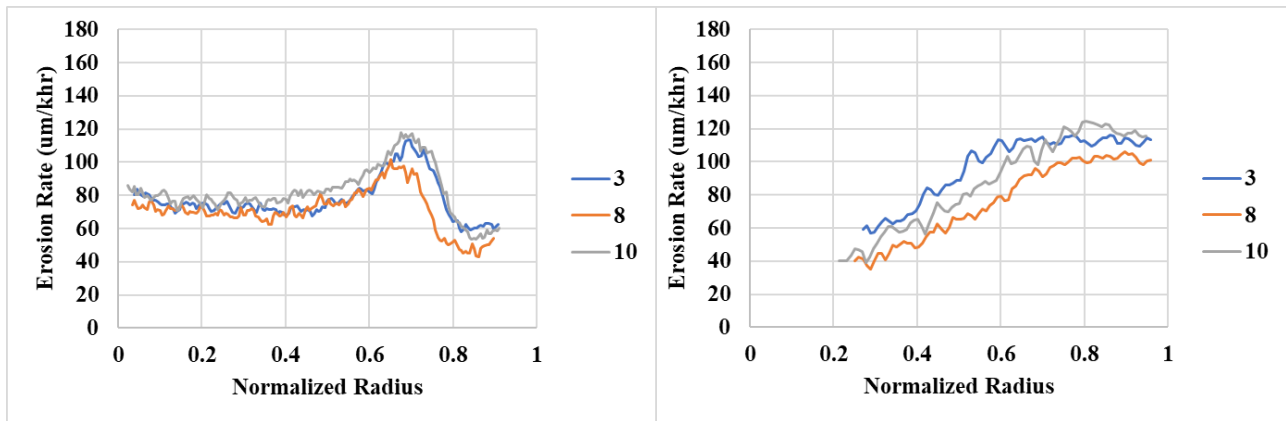


Figure 7. Subtraction method erosion rates for SDWT-3 (900 W 350 V, 5 μ torr-Xe). Left: IFPC, Right: OFPC.

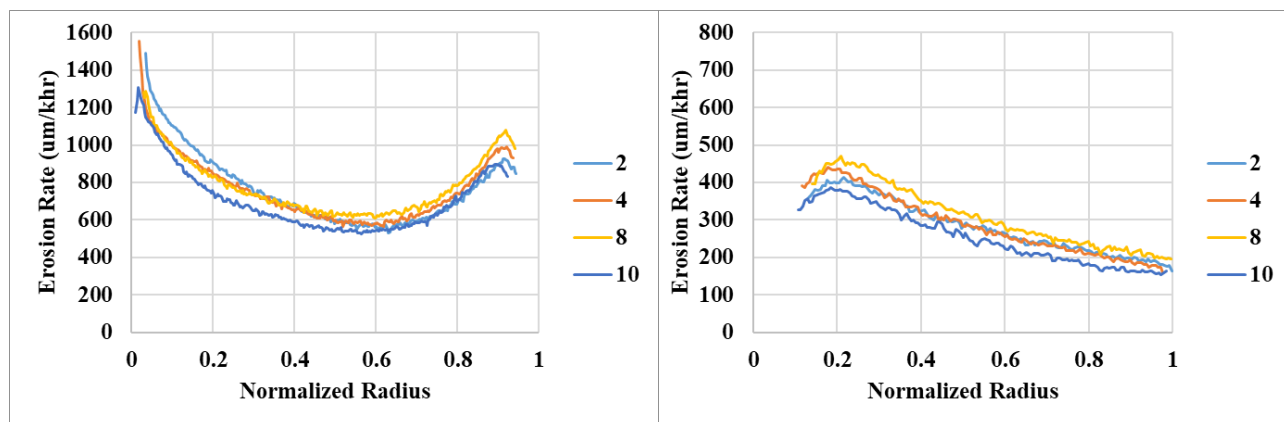


Figure 8. Subtraction method erosion rates for SDWT-Kr (900 W 250 V, 7 μ torr-Kr). Left: IFPC, Right: OFPC.

IV. Discussion of Results

A. Discrepancy between Measurement Methods

Across all xenon erosion data collected, there is significantly more variation between the masking method and the subtraction method than there is between the different throttle conditions and background pressures tested. The overall erosion profiles determined by both methods are similar, but in all tests, erosion rates calculated via the subtraction method are approximately 30-40 $\mu\text{m}/\text{chr}$ higher than those calculated via the masking method on both the IFPC and OFPC. It is unclear why this is the case. For SDWTs 1 and 2, the same Nanovea profilometer was used for both the masking method and subtraction method data, which suggests the discrepancy is not due to the profilometer used. This is also supported by the fact that subtraction-method erosion rates for SDWTs 2 and 3 are not significantly different, where SDWT-3 data was taken on the Keyence profilometer.

It is possible that the accumulation of material from facility backsputtering around the edges of the pole cover masks, which occurred in all tests, contributes to the discrepancy. It is unlikely, however, that material build-up due to sputtering of fastener material is the cause, because this deposition is clearly local in the SDWT-3 data and is not present in the other SDWTs because smaller fasteners were used. Additionally, the OFPC masks are farther removed from the fasteners, but the discrepancy is still present in the OFPC data.

While there has been no formal uncertainty quantification for the subtraction method as applied to these data sets, the authors deem the subtraction method erosion data for the NGHT-1X as more trustworthy than the data obtained using the masking method, for several reasons. For one, there is the known issue of material accumulation underneath the edges of the masks, which made clean measurements more difficult. Additionally, similar erosion rate profiles were obtained using both the Nanovea and Keyence profilometers, which suggests that neither random nor systematic error are substantially affecting the results. Therefore, in the following comparisons between datasets, all comparisons are made using the subtraction method data.

It is worth noting that the masking method and associated uncertainty analysis utilized here for calculating Hall thruster erosion was developed for the 12.5 kW HERMeS (now AEPS) thruster program [14]. This thruster is significantly larger than the NGHT-1X, so it is possible that certain factors systematically influence the masking method results on a smaller thruster in a way that does not impact larger thrusters. Interestingly, a similar discrepancy has been reported on the MaSMi thruster, another 1 kW-class magnetically shielded Hall thruster, where erosion rates calculated via the masking method underpredicted erosion rates observed during the long duration wear test [16]. However, the root cause may be different in each case.

While the masking method results for the NGHT-1X are questionable, this does not necessarily imply that the masking method itself is flawed in other applications such as HERMeS/AEPS. A more systematic evaluation of both masking method and subtraction method results over multiple thrusters would be required to fully assess the adequacy and applicability of the masking method for measuring Hall thruster erosion, or to determine best practices which ensure reliable results in all cases.



Figure 9. Photo of the NGHT-1X Long Duration Wear Test unit after 873 hours of operation.

B. Comparison between 700 W 300 V and 900 W 350 V

As previously mentioned, no pre-test scan was taken for SDWT-1 at 700 W 300 V, but rather the nominal design dimensions were used. The primary insight to be gained from the SDWT-1 data is the amplitude of the IFPC erosion peak relative to the other regions of the IFPC. This peak is 50-60 $\mu\text{m}/\text{hr}$ higher than the erosion rates closer to the cathode (Figure 5), whereas in SDWT-2 at 900 W 350 V, the peak is 70-80 $\mu\text{m}/\text{hr}$ higher than erosion rates elsewhere (Figure 6). However, as stated in an earlier section, SDWT-1 started with non-chamfered pole covers, whereas all other SDWTs started with chamfered pole covers to represent some amount of erosion. Therefore, it is unclear how much of the difference between SDWT-1 and SDWT-2 is due to the difference in throttle condition or the difference in initial state of the pole covers. If nothing else, the data shows that there is no fundamental difference in erosion patterns between 700 W 300 V and 900 W 350 V, but rather that they follow similar distributions.

C. Effect of Background Pressure

More interesting is the comparison between SDWT-2 and SDWT-3, which shows the difference in erosion at 900 W 350 V at 12 $\mu\text{torr-Xe}$ (SDWT-2, Figure 6) versus 5 $\mu\text{torr-Xe}$ (SDWT-3, Figure 7). The main difference in erosion rates between these two tests is in the region of the IFPC between the central cathode and the erosion peak at $R = 0.7$. At the higher background pressure, erosion rates in this region averaged 50 $\mu\text{m}/\text{hr}$, whereas erosion rates in the same region at the lower background pressure averaged 50% higher at 75 $\mu\text{m}/\text{hr}$. This is especially interesting when looking at the rest of the erosion distribution; the erosion peak on the IFPC and the entire erosion profile on the OFPC show minimal difference between both tests.

The most plausible explanation of this result is that the erosion peak on the IFPC and the erosion on the entire OFPC are caused by one population of ions, whereas the rest of the IFPC erosion is caused by a separate population of ions. The most recent experimental and numerical investigations of pole cover erosion in magnetically shielded Hall thrusters have shown the importance of cross-stream ion instabilities in the IFPC region leading to anomalous heating of ions generated in that region, which results in increased erosion rates [10,17,18,19]. In addition to erosion from these ions, there is also erosion caused by ions originating in or near the main discharge, which strike the pole cover with higher energy than ions created and heated in the IFPC region [7,9].

It is plausible that the sensitivity to background pressure is different for each of these mechanisms, such that when going from 12 $\mu\text{torr-Xe}$ to 5 $\mu\text{torr-Xe}$, the generation and acceleration of eroding ions from the beam did not appreciably change, whereas the conditions driving the cross-stream instabilities in the IFPC region changed enough to substantially increase erosion rates. However, it is also possible that the different sensitivities of erosion from each population are

driven not by background pressure but by facility configuration. Wear testing of the HERMeS 12.5 kW thruster has shown that erosion rates in one facility with varying background pressure (controlled by auxiliary injection of xenon) are similar across different pressures, whereas erosion in a different facility was substantially different despite having roughly equivalent pressure to the other tests [20]. It may be that the variation observed between SDWT-2 and SDWT-3 was not driven by background pressure but rather by facility configuration differences. Because the NGHT-1X utilizes non-conductive pole covers, it is likely less susceptible to erosion variability driven by electrical configuration versus a thruster like HERMeS which uses conductive pole covers. However, further experimental and numerical work would be required to determine the driving factor(s).

Regardless, the hypothesis of two separate eroding populations in the NGHT-1X erosion profile is supported by the measurements and is further supported by visual evidence from the ongoing Long Duration Wear Test (LDWT) of the NGHT-1X, which began in August 2023 and will be the subject of a future publication. Figure 9 shows a photo of the LDWT thruster after completion of the first 873 hours of the test. It is commonly observed in Hall thruster wear tests that striations or ridges form along the discharge channel walls and adjacent pole cover edges as they erode [21]. Interestingly, the NGHT-1X LDWT unit shows striations which continue along the front-facing surface of the pole covers. This was also observed in each SDWT, but they are more visually apparent after the first LDWT segment which was almost double the length of any SDWT. There is an important feature of interest of these pole cover striations; while they are present across the entire OFPC and in the IFPC erosion peak, they are absent on the rest of the IFPC. Put another way, the striations are present in locations where erosion showed little sensitivity to background pressure, but where higher sensitivity to background pressure was observed, the IFPC surface is smooth. This further supports the hypothesis that the erosion caused by ions originating in or near the beam (which would travel in the radial direction at high velocity and plausibly cause the radial striations observed on the LDWT unit) show little to no sensitivity to background pressure when going from 12 μ torr-Xe to 5 μ torr-Xe, whereas erosion caused by ions created and anomalously heated in the IFPC region (which would have no strong radial velocity component and therefore would plausibly result in a smooth eroded surface) do show a strong sensitivity to background pressure in the tested range.

These results naturally beg the question of whether 5 μ torr-Xe is sufficiently low to reproduce the erosion rates that occur in the space environment, or if erosion rates would continue to increase when going from 5 μ torr-Xe to the space environment. Additional testing is required to resolve this question. However, the NGHT-1X has already undergone performance and plume testing in \sim 12 μ torr-Xe (VF-8), \sim 5 μ torr-Xe (VF-11), and \sim 1 μ torr-Xe (VF-5) environments. Presenting these results is beyond the scope of this paper. There is a clear, though slight, change in performance when going from \sim 12 μ torr-Xe to \sim 5 μ torr-Xe, indicated by a change to both the measured thrust and the ratio of discharge current to flow rate, the latter of which is measurable to higher precision than thrust and therefore serves as a more reliable indication of performance change. On the other hand, when going from \sim 5 μ torr-Xe to \sim 1 μ torr-Xe, at all throttle conditions, there is no discernable change in either thrust or the ratio of discharge current to flow rate. While it is almost certain that performance and erosion have different sensitivities to background pressure, these results support the notion that erosion rates would not significantly change below 5 μ torr-Xe, though further testing is required to verify this.

D. Comparison between Xenon and Krypton

The results of the krypton SDWT stand in stark contrast to the erosion rates measured on xenon propellant. Erosion rates on the OFPC and IFPC increased roughly by factors of 5 and 10 respectively. There are some features of the krypton erosion distribution that are similar to those on xenon, and some that are new. Similar to xenon erosion, Figure 8 shows that both the IFPC and OFPC have peaks at certain radial locations. However, the peaks in the krypton erosion distribution are much closer to the discharge channel compared to the xenon erosion peaks. The locations of the peaks show more resemblance to the erosion distributions measured on the HERMeS 12.5 kW Hall thruster [12], whose magnetic field distribution pushes the plasma discharge further downstream than the NGHT-1X [8]. Near-field plume measurements of the same thruster on xenon and krypton have shown that when operating on krypton, the acceleration region is longer and further downstream than when operating on xenon [22]. Therefore, it is not surprising that the erosion distribution of the NGHT-1X operating on krypton resembles the erosion distribution of a more magnetically shielded thruster operating on xenon.

In addition to the change in location of the IFPC and OFPC erosion peaks, there is a strong peak in IFPC erosion near the cathode, which is absent from the xenon erosion data. Measurements taken of the 12.5 kW HERMeS thruster at a variety of throttle conditions show that in some cases there is a prominent erosion peak near the cathode, whereas in

other cases it is entirely absent [11]. The results in [11] show that the cathode can be a major source of eroding ions in certain operating modes. It is likely that the operating conditions used for SDWT-Kr resulted in unfavorable cathode behavior which led to extreme erosion rates near the cathode.

No radial striations are observed on either the IFPC or OFPC after SDWT-Kr. However, the test was only 290 hours, so it's possible that striations would have appeared on the top-facing surfaces of the thruster after a longer duration.

At first glance, these results seem to pose a serious problem for any potential high delta-V application of a krypton-fueled Hall thruster. In fact, with these measured erosion rates, it is possible that longer lifetimes could be achieved more easily with a completely unshielded Hall thruster. However, there are several potential ways to reduce the erosion rates on krypton.

For one, the 900 W 250 V throttle condition was chosen for SDWT-Kr due to the thermal performance of the unit under test. Operation on krypton results in significantly higher heat loading on the thruster; the 900 W 250 V condition resulted in temperatures 50+ °C higher than the nominal max power condition of the NGHT-1X on xenon. Running at a higher power condition would have increased the likelihood of failure of the magnet coils or other components. However, performance testing over a range of throttle conditions on krypton (which is the subject of a separate paper) showed that at higher current densities, thruster operation improved significantly in terms of discharge stability and performance, at the cost of heat loads that are untenable for long-term operation. With an improved thermal design, higher current densities would be accessible to the thruster which could result in reduced erosion rates, particularly near the cathode.

Additionally, the erosion rates could be further reduced by switching to graphite pole covers instead of alumina. Testing of the 12.5 kW HERMeS thruster at the same throttle condition using both alumina and graphite pole covers shows that erosion rates with alumina are as much as six times higher than erosion rates with graphite [12]. Assuming the cathode erosion peak can be mitigated by optimizing the thruster for the desired throttle condition, this reduction would bring the NGHT-1X erosion rates on krypton down to only 67% higher than xenon erosion rates. While still higher than desirable, these erosion rates would be manageable and could potentially serve the same missions as a xenon-fueled NGHT-1X in terms of required total impulse. Pole covers made from a conductive material pose their own challenges for thruster operation and spacecraft integration, but these challenges can be managed if they are required for a long-life krypton Hall thruster.

V. Conclusions

During the development phase of the NGHT-1X, several Short Duration Wear Tests were performed to assess the lifetime capability of the thruster in support of the Mission Extension Pod mission, as well as potential future missions using krypton propellant. These data sets provide an interesting comparison of erosion rates between throttle conditions, background pressure, and propellant.

Firstly, the data collected indicates a discrepancy between the masking method that is typically used for measuring pole cover erosion in Hall thrusters and other methods for measurement. This discrepancy is likely exacerbated by the small size and particular design features of the NGHT-1X, and therefore does not necessarily imply that results obtained with this method on other thrusters are questionable. Regarding the observed erosion trends, results indicate that erosion from ions heated by cross-stream instabilities in the IFPC region show a different sensitivity to background pressure compared to ions originating in or near the main discharge.

Additionally, the results of the krypton SDWT show that NGHT-1X erosion rates on krypton at the throttle condition tested are significantly higher than all measured erosion using xenon. This poses a challenge for high delta-V applications of the NGHT-1X using krypton propellant, but there are paths to reduce erosion in order to enable these mission applications.

In all the xenon wear tests performed, the measured erosion rates indicate an NGHT-1X lifetime capability in excess of 16,000 hours, or 3.3 MNs total impulse at 900 W 350 V, which supports the MEP mission with margin as well as many other potential applications on small- to medium-sized spacecraft. The Long Duration Wear Test of the NGHT-1X began in August 2023 and will continue into 2025 to demonstrate the full total impulse requirement. The LDWT will be the subject of a future paper, but thus far the results support the conclusions made from these SDWTs.

Acknowledgements

SDWT-1 was funded by the NASA Space Technology Mission Directorate Game Changing Division Program through the 2020 Announcement of Collaborative Opportunity award given to Northrop Grumman. SDWTs 2 and 3 were funded by the NASA Human Exploration and Operations Mission Directorate (now Space Operations Mission Directorate) through the 2014 Collaborations for Commercial Space Capabilities award SAA-QA-14-18881. Lastly, the krypton SDWT was funded by Northrop Grumman through an Umbrella Space Act Agreement, SAA3-1724.

References

- [1] Nikrant, A. W., Glogowski, M. J., Cochran, D. E., Moquin, T., Choi, Y. E., Benavides, G. F., Kamhawi, H., Sarver-Verhey, T. R., Baird., M. J., Rhodes, C. R., and Mackey, J. A., “Overview and Performance Characterization of Northrop Grumman’s 1 kW Hall Thruster String”, 37th International Electric Propulsion Conference, Boston, MA, USA, June 2022.
- [2] Benavides, G. F., Kamhawi, H., Sarver-Verhey, T. R., Rhodes, C. R., Baird., M. J., and Mackey, J. A., “High-Propellant Throughput Sub-kW Electric Propulsion System for Deep Space Science and Exploration”, 37th International Electric Propulsion Conference, Boston, MA, USA, June 2022.
- [3] Kamhawi, H., Liu, T. M., Benavides, G. F., Mackey, J. A., Sarver-Verhey, T. R., Yim, J., Butler-Craig, N. I., and Myers, J., “Performance, Stability, and Thermal Characterization of a Sub-Kilowatt Hall Thruster”, 36th International Electric Propulsion Conference, Vienna, Austria, September 2019.
- [4] De Grys, K., Mathers, A., Welander, B., and Khayms, V., “Demonstration of 10,400 Hours of Operation on a 4.5 kW Qualification Model Hall Thruster”, 46th AIAA/ASME/SAE/ASEE Joint Propulsion Conference & Exhibit, July 2010, Nashville, TN, USA.
- [5] Mikellides, I. G., Katz, I., Hofer, R. R., Goebel, D. M., de Grys, K., and Mathers, A., “Magnetic Shielding of the Acceleration Channel Walls in a Long-Life Hall Thruster”, 46th AIAA/ASME/SAE/ASEE Joint Propulsion Conference & Exhibit, July 2010, Nashville, TN, USA.
- [6] Mikellides, I. G., and Lopez Ortega, A., “Assessment of Pole Erosion in a Magnetically Shielded Hall Thruster”, 50th AIAA/ASME/SAE/ASEE Joint Propulsion Conference, July 2014, Cleveland, OH, USA.
- [7] Jorns, B. A., Dodson, C., Anderson, J., Goebel, D. M., Hofer, R. R., Sekerak, M., Lopez Ortega, A., and Mikellides, I., “Mechanisms for Pole Piece Erosion in a 6-kW Magnetically-Shielded Hall Thruster”, 52nd AIAA/SAE/ASEE Joint Propulsion Conference, July 2016, Salt Lake City, UT, USA.
- [8] Kamhawi, H., Mackey, J., Frieman, J., Huang, W., Gray, T., Haag, T., and Mikellides, I., “HERMeS Thruster Magnetic Field Topology Optimization Study: Performance, Stability, and Wear Results”, 36th International Electric Propulsion Conference, Vienna, Austria, 2019.
- [9] Lopez Ortega, A., Mikellides, I. G., Conversano, R., Lobbia, R. B., and Chaplin, V. H., “Plasma Simulations for the Assessment of Pole Erosion in the Magnetically Shielded Miniature Hall Thruster (MaSMi)”, 36th International Electric Propulsion Conference, Vienna, Austria, 2019.
- [10] Lopez Ortega, A., Mikellides, I. G., Chaplin, V. H., Huang, W., and Frieman, J. D., “Anomalous Ion Heating and Pole Erosion in the 12.5-kW Hall Effect Rocket with Magnetic Shielding (HERMeS)”, AIAA Propulsion and Energy 2020 Forum, August 2020.
- [11] Polk, J. E., Lobbia, R., Barriault, A., Guerrero, P., Mikellides, I., Lopez Ortega, A., “Inner Front Pole Cover Erosion in the 12.5 kW HERMeS Hall Thruster Over a Range of Operating Conditions”, 35th International Electric Propulsion Conference, Atlanta, GA, USA, 2017.
- [12] Frieman, J. D., Gilland, J. H., Kamhawi, H., Mackey, J., Williams Jr., G. J., Hofer, R. R., and Peterson P. Y., “Wear trends of the 12.5 kW HERMeS Hall thruster”, Journal of Applied Physics 130, 143303, 2021.
- [13] Lobbia, R. B., Conversano, R. W., Lopez Ortega, A., Reilly, S., and Mikellides, I. G., “Pole Erosion Measurements for the Development Model of the Magnetically Shielded Miniature Hall Thruster (MaSMi-DM)”, 36th International Electric Propulsion Conference, Vienna, Austria, 2019.
- [14] Mackey, J., Frieman, J., Ahern, D., and Gilland, J., “Uncertainty in Electric Propulsion Erosion Measurements”, AIAA Propulsion and Energy 2019 Forum, August 2019.
- [15] Frieman, J. D., Kamhawi, H., Huang, W., Mackey, J., Ahern, D. M., Peterson, P. Y., Gilland, J., Hall, S. J., Hofer,

- R. R., Inaba, D., Dao, H., Zubair, J., Neuhoff, J., and Branch, N. A., “Wear Test of the 12.5-kW Advanced Electric Propulsion System Engineering Test Unit Hall Thruster”, AIAA Propulsion and Energy 2020 Forum, August 2020.
- [16] Chaplin, V. H., Simmonds, J. B., Byrne, M. P., Goebel, D. M., Lopez Ortega, A., Lobbia, R. B., Mikellides, I. G., Hofer, R. R., Zhu, B. X., Ratliff, J. M., and Conversano, R. W., “Extended Life Qualification of the Magnetically Shielded Miniature (MaSMi) Hall Thruster”, 37th Annual Small Satellite Conference, Logan, UT, 2023.
- [17] Mikellides, I. G. and Lopez Ortega, A., “The Dispersion of the Modified Two-Stream and Lower Hybrid Drift Instabilities in the Near-pole Plume of a Magnetically Shielded Hall Thruster”, AIAA Propulsion and Energy 2021 Forum, August 2021.
- [18] Lopez Ortega, A. and Mikellides, I. G., “Validation of Hall2De simulations with anomalous ion heating in the pole region of a magnetically shielded Hall thruster”, 37th International Electric Propulsion Conference, Boston, MA, USA, June 2022.
- [19] Mikellides, I. G., Lopez Ortega, A., Lobbia, R. B., and Chaplin, V. H., “The Dispersion of Lower-Hybrid Instabilities and Comparisons with Measurements Near the Front Pole of a Magnetically Shielded Hall Thruster”, AIAA SCITECH 2023 Forum, National Harbor, MD, USA, January 2023.
- [20] Frieman, J. D., Kamhawi, H., Peterson, P. Y., Herman, D., Gilland, J., and Hofer, R., “Impact of Facility Pressure on the Wear of the NASA HERMeS Hall Thruster”, 36th International Electric Propulsion Conference, Vienna, Austria, 2019.
- [21] Brown, N. P. and Walker, M. L. R., “Review of Plasma-Induced Hall Thruster Erosion”, Appl. Sci. 2020, 10(11), 3775, May 2020.
- [22] Linnell, J. A. and Gallimore, A. D., “Internal plasma potential measurements of a Hall thruster using xenon and krypton propellant”, Phys. Plasmas 13, 093502, September 2006.